LETTER **Communicated by Jesus Cortes**

Downstream Effect of Ramping Neuronal Activity through Synapses with Short-Term Plasticity

Wei Wei
ww41@nyu.edu
Center for Neural Science, New York University, New York, NY 10003, U.S.A.

Xiao-Jing Wang
xjwang@nyu.edu
Center for Neural Science, New York University, New York, NY 10003, U.S.A., and NYU-ECNU Joint Institute of Brain and Cognitive Science, NYU Shanghai, Shanghai, China.

Ramping neuronal activity refers to spiking activity with a rate that increases quasi-linearly over time. It has been observed in multiple cortical areas and is correlated with evidence accumulation processes or timing. In this work, we investigated the downstream effect of ramping neuronal activity through synapses that display short-term facilitation (STF) or depression (STD). We obtained an analytical result for a synapse driven by deterministic linear ramping input that exhibits pure STF or STD and numerically investigated the general case when a synapse displays both STF and STD. We show that the analytical deterministic solution gives an accurate description of the averaging synaptic activation of many inputs converging onto a postsynaptic neuron, even when fluctuations in the ramping input are strong. Activation of a synapse with STF shows an initial cubical increase with time, followed by a linear ramping similar to a synapse without STF. Activation of a synapse with STD grows in time to a maximum before falling and reaching a plateau, and this steady state is independent of the slope of the ramping input. For a synapse displaying both STF and STD, an increase in the depression time constant from a value much smaller than the facilitation time constant τ_F to a value much larger than τ_F leads to a transition from facilitation dominance to depression dominance. Therefore, our work provides insights into the impact of ramping neuronal activity on downstream neurons through synapses that display short-term plasticity. In a perceptual decision-making process, ramping activity has been observed in the parietal and prefrontal cortices, with a slope that decreases with task difficulty. Our work predicts that neurons downstream from such a decision circuit could instead display a firing plateau independent of the task difficulty, provided that the synaptic connection is endowed with short-term depression.

Neural Computation **28, 652–666** (2016)
doi:10.1162/NECO_a_00818

1 Introduction

Ramping neuronal activity has been observed in different cortical and subcortical areas, such as lateral intraparietal cortex, frontal eye field, superior colliculus, thalamus, and presupplementary and supplementary motor areas, and it provides a neuronal implementation of the evidence accumulation process during perceptual decision making (Wang 2002, 2008; Gold & Shadlen, 2007) and timing (Komura et al., 2001; Reutimann, Yakovlev, Fusi, & Senn, 2004; Mita, Mushiake, Shima, Matsuzaka, & Tanji, 2009; Simen, Balci, de Souza, Cohen, & Holmes, 2011; Merchant, Harrington, & Meck, 2013). A simple mathematical model for the ramping neuronal activities is the drift-diffusion model (Hanes & Schall, 1996; Huk & Shadlen, 2005; Ratcliff, Cherian, & Segraves, 2003). Neurons in the caudate nucleus (the eye movement part of the striatum) have been observed to show a ramping activity followed by a saturation before saccade initiation (Ding & Gold, 2010). The striatum receives direct projections from cortical areas that display ramping neuronal activity. The origin of the saturation of ramping activity in the striatum is not yet well understood.

Short-term plasticity (STP) is a common feature of cortical synapses, and both short-term facilitation (STF) and depression (STD) have been observed in the cortex (Abbott & Regehr, 2004; Morrison, Diesmann, & Gerstner, 2008). In the phenomenological model of STP, depression is attributed to a decrease of vesicle availability, while facilitation is attributed to an increase of vesicle release probability (Tsodyks & Markram, 1997; Tsodyks, Pawelzik, & Markram, 1998; Fuhrmann, Segev, Markram, & Tsodyks, 2002; Hempel, Hartman, Wang, Turrigiano, & Nelson, 2000). For simplicity in theoretical understanding of the role of synaptic plasticity, depression or facilitation alone was often considered, although in general, both depression and facilitation coexist in a synapse. In experimental and theoretical investigations, presynaptic input with a constant rate is usually applied. In previous work, we proposed that the saturation of striatal ramping during evidence accumulation could be explained by STD in the corticostriatal synapses (Wei, Rubin, & Wang, 2015). In this work, we analytically characterized the downstream effect of synapses displaying STF or STD driven by fluctuating ramping presynaptic inputs described by the drift-diffusion model. We also investigated the general case when both STF and STD coexist in a synapse numerically.

2 Phenomenological Model for STP

In the phenomenological model for STP, the activity of a synapse with pure STF is described as

$$\frac{dF}{dt} = \alpha(1-F)\sum_j \delta(t-t^j) - \frac{F}{\tau_F}, \tag{2.1}$$

$$\frac{ds}{dt} = F \sum_j \delta(t - t^j) - \frac{s}{\tau_a}, \tag{2.2}$$

where t^j is the time of the jth presynaptic input spike, F represents the vesicle release probability, and s is the gating variable. When a presynaptic spike arrives, F first increases with an amount $\alpha(1 - F)$, and then decays with a time constant τ_F during the intervals of input spikes. The gating variable s is then updated following the update of F, with an increment of F. The conductance to a postsynaptic neuron is given by the product of the gating variable s and a constant synaptic efficacy.

The presynaptic spike train in equations 2.1 and 2.2 represents the instantaneous input firing rate $r(t)$, that is, $r(t) \simeq \sum_j \delta(t - t^j)$. Here we are interested in the case when $r(t)$ describes a ramping input rate as observed for cortical neurons in multiple brain areas. The ramping input rate $r(t)$ is well described by the classical drift-diffusion model,

$$\tau \frac{dr}{dt} = \mu + \sigma\sqrt{\tau}\eta(t), \tag{2.3}$$

where τ is the time constant for the drift-diffusion process, μ is the drift term, $\eta(t)$ is a gaussian white noise satisfying $\langle \eta(t) \rangle = 0$ and $\langle \eta(t)\eta(t') \rangle = \delta(t - t')$, and σ is the noise strength. We will take $\tau = 10$ ms, but all the results will not depend on the exact value of τ. The synaptic dynamics are given by the following equations,

$$\frac{dF}{dt} = \alpha(1 - F)r(t) - \frac{F}{\tau_F}, \tag{2.4}$$

$$\frac{ds}{dt} = Fr(t) - \frac{s}{\tau_a}. \tag{2.5}$$

We will use $\tau_a = 2$ ms, $\tau_F = 400$ ms, and $\alpha = 0.25$. The value for τ_a is characteristic of the decay time constant for AMPAergic synapses. Different values of τ_F and α (with $\tau_F \gg \tau_a$) will not qualitatively change the behavior of the phenomenological model.

For a synapse with pure STD, the synaptic dynamics are described as

$$\frac{dD}{dt} = -pD \sum_j \delta(t - t^j) + \frac{1 - D}{\tau_D}, \tag{2.6}$$

$$\frac{ds}{dt} = pD \sum_j \delta(t - t^j) - \frac{s}{\tau_a}, \tag{2.7}$$

where p is a constant vesicle release probability and D represents the fraction of available vesicles. At the arrival of a presynaptic spike, D is first reduced

by an amount pD and then recovered with a time constant τ_D during the intervals of input spikes. The gating variable s is then updated following the update of D, with an increment of pD.

Replacing the presynaptic spike train by the instantaneous input rate $r(t)$ described by equation 2.3, we have the following equations:

$$\frac{dD}{dt} = -pr(t)D + \frac{1-D}{\tau_D}, \tag{2.8}$$

$$\frac{ds}{dt} = pr(t)D - \frac{s}{\tau_a}. \tag{2.9}$$

We will use $p = 0.45$ and $\tau_D = 600$ ms. Different values of p and τ_D (with $\tau_D \gg \tau_a$) will not qualitatively change the behavior of the phenomenological model.

We first study a deterministic linear ramping input ($\sigma = 0$ case) and then consider a general fluctuating ramping input described by the drift-diffusion model . The initial values of F, D, and s at $t = 0$ are denoted as F_0, D_0, and s_0. We will use $F_0 = 0$, $D_0 = 1$, and $s_0 = 0$ unless stated otherwise.

3 Deterministic Linear Ramping Input

3.1 Synapse with STF. When $\sigma = 0$ in equation 2.3, the input rate ramps up linearly with time (i.e., $r = kt$), where $k \equiv \mu/\tau$ is the slope of ramping. Equations 2.4 and 2.5 can be solved analytically,

$$F = 1 - \exp\left(-\frac{1}{2}\alpha k t^2 - \frac{t}{\tau_F}\right)\left(1 - F_0 - \frac{1}{\tau_F}\sqrt{\frac{2}{\alpha k}}\mathcal{F}\left(\frac{1}{\tau_F\sqrt{2\alpha k}}\right)\right)$$
$$-\frac{1}{\tau_F}\sqrt{\frac{2}{\alpha k}}\mathcal{F}\left(\sqrt{\frac{\alpha k}{2}}t + \frac{1}{\tau_F\sqrt{2\alpha k}}\right) \tag{3.1}$$

$$s \simeq k\tau_a F t, \tag{3.2}$$

where $\mathcal{F}(x)$ is the Dawson's integral (Abramowitz & Stegun, 1970) as defined in the appendix.

In Figure 1, the synaptic dynamics for ramping input with two different slopes and constant input (see Figure 1A) are illustrated and are compared with the control case when there is no STP (see Figure 1B). The activities of F and s for a synapse with STF are shown in Figures 1C and 1D. When t is small, we have

$$F \simeq \frac{1}{2}\alpha k t^2, \tag{3.3}$$

$$s \simeq \frac{1}{2}\alpha\tau_a k^2 t^3. \tag{3.4}$$

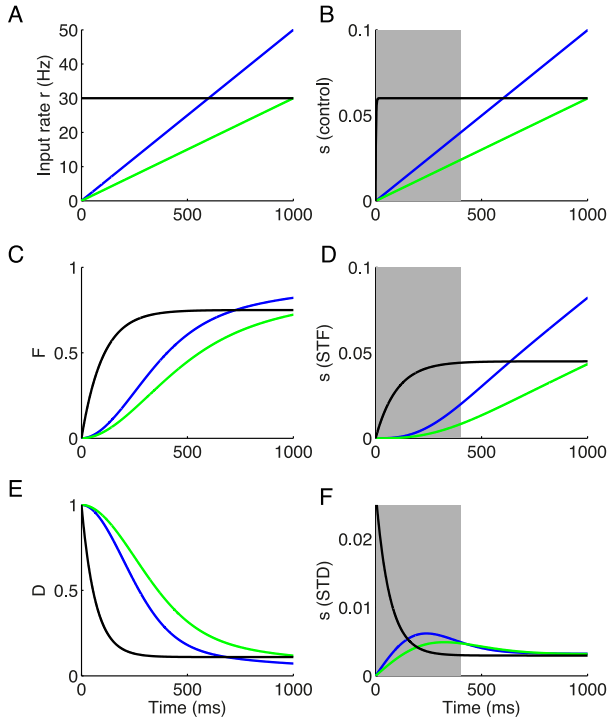

Figure 1: Activation level of a synapse with pure STF or STD. (A) The input rate ramps up linearly, with slope $k = 30$ (green) and 50 (blue) (in sec^{-2}). The black curve represents a constant input with rate 30 Hz. (B) The activation level of the gating variable s in the control case when there is no STP. (C,D) The facilitation factor F (C) and the activation level s (D) for a synapse with pure STF. (E,F) The depression factor D (E) and activation level s (F) for a synapse with pure STD. The gray shaded areas (with width τ_F) highlight the different activity of s for a synapse with and without STP. Parameters used: $\tau_a = 2$ ms, $\tau_F = 400$ ms, $\alpha = 0.25$, $\tau_D = 600$ ms, $p = 0.45$.

When t is large, we have

$$F \simeq 1 - \frac{1}{\alpha \tau_F k t + 1} \to 1, \tag{3.5}$$

$$s \simeq \frac{\alpha \tau_a \tau_F k^2 t^2}{\alpha \tau_F k t + 1} \to \tau_a k t. \tag{3.6}$$

Therefore, when t is large, the facilitation factor F will saturate hyperbolically for a ramping input, while for a constant input, it will reach its stationary state exponentially (see Figure 1C and the appendix). The gating

variable s will increase cubically at the initial period (gray region in Figure 1D, with width τ_F), then is followed by a linear increase similar to the control case (see Figure 1B). Note that for a constant input rate, s will saturate when t is large in the timescale τ_F for a synapse with STF (see Figure 1D, black curve), while in the control case, s will saturate to its steady state in the much shorter timescale τ_a (see Figure 1B, black curve).

3.2 Synapse with STD. For $r = kt$ and $\sigma = 0$, from equations 2.8 and 2.9, we have

$$D = \frac{1}{\tau_D}\sqrt{\frac{2}{kp}}\mathcal{F}\left(\sqrt{\frac{kp}{2}}t + \frac{1}{\tau_D\sqrt{2kp}}\right) + \left(D_0 - \frac{1}{\tau_D}\sqrt{\frac{2}{kp}}\mathcal{F}\left(\frac{1}{\tau_D\sqrt{2kp}}\right)\right)\exp\left(-\left(\frac{1}{2}pkt^2 + \frac{t}{\tau_D}\right)\right), \tag{3.7}$$

$$s \simeq pk\tau_a Dt. \tag{3.8}$$

When t is large,

$$D \simeq \frac{1}{\tau_D}\sqrt{\frac{2}{kp}}\frac{1}{2(\sqrt{\frac{kp}{2}}t + \frac{1}{\tau_D\sqrt{2kp}})} = \frac{1}{kp\tau_D t + 1} \to \frac{1}{kp\tau_D t}, \tag{3.9}$$

$$s \to \frac{\tau_a}{\tau_D}. \tag{3.10}$$

We see that for the ramping input, D decays hyperbolically for large t, which is slower than that for a constant input rate that decays exponentially to its steady state (see Figure 1E). The gating variable s will reach a steady state, which is independent of the ramping slope k and release probability p (see Figure 1F). Note that the steady state for a ramping input is the same as that for a constant input when the constant rate is large enough, as given in the appendix.

Before reaching its steady state, the gating variable s for a synapse with STD will develop a maximum when receiving ramping input (see Figure 1F). Although the steady state of s is independent of the ramping slope k and the release probability p, the maximal value of s depends on both k and p. For small t and applying equation A.3,

$$D \simeq \frac{1}{\tau_D}\sqrt{\frac{2}{kp}}\left(\sqrt{\frac{kp}{2}}t + \frac{1}{\tau_D\sqrt{2kp}}\right) + \left(1 - \frac{1}{kp\tau_D^2}\right)\left(1 - \frac{t}{\tau_D} - \frac{1}{2}kpt^2\right) = 1 + \frac{t}{kp\tau_D^3} - \frac{1}{2}kpt^2\left(1 - \frac{1}{kp\tau_D^2}\right), \tag{3.11}$$

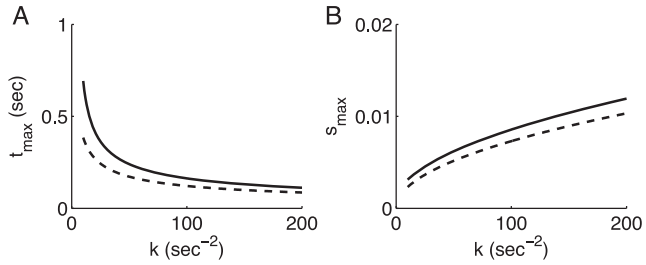

Figure 2: The maximal activation level and the time for reaching the maximum for a synapse with only STD as a function of ramping slope. (A) The time for reaching the maximum of s as a function of the ramping slope k. (B) The maximal value of s as a function of the ramping slope k. The dashed lines in panels A and B are approximations from equations 3.14 and 3.15, respectively.

where $\frac{1}{kp\tau_D^2}$ (~ 0.1) is small, so we have

$$D \simeq 1 - \frac{1}{2}kpt^2. \tag{3.12}$$

By comparing equation 3.12 with equation A.9 in the appendix, we see the different small time behaviors of D for ramping and constant input rates (see Figure 1 E). Therefore, when t is small (but $t > \tau_a$),

$$s \simeq pk\tau_a t \left(1 - \frac{1}{2}pkt^2\right), \tag{3.13}$$

which has a maximal value at time $t_{\max}$ given by

$$t_{\max} = \sqrt{\frac{2}{3}}\frac{1}{\sqrt{pk}}, \tag{3.14}$$

$$s_{\max} = \sqrt{\frac{8}{27}}\sqrt{pk}\,\tau_a. \tag{3.15}$$

Figures 2A and 2B compare the approximate and real values of $t_{\max}$ and $s_{\max}$ as a function of k, respectively. We see that equations 3.14 and 3.15 provide qualitative information about the location and value of the maximum of s: a ramping input with a higher slope k will have a larger maximum developed within a shorter time.

3.3 Synapse with Both STF and STD. In general, both STF and STD are coexisting in a synapse, with the dynamics described by Tsodyks et al.

(1998), Hempel et al. (2000), and Lindner, Gangloff, Longtin, and Lewis (2009):

$$\frac{dF}{dt} = \alpha r(t)(1-F) - \frac{F}{\tau_F}, \tag{3.16}$$

$$\frac{dD}{dt} = -r(t)FD + \frac{1-D}{\tau_D}, \tag{3.17}$$

$$\frac{ds}{dt} = r(t)FD - \frac{s}{\tau_a}. \tag{3.18}$$

For a deterministic linear input rate, $r = kt$, the solution of equation 3.16 is given by equation 3.1. Since τ_a is much smaller than τ_F and τ_D, equation 3.18 is simplified to

$$s \simeq k\tau_a FDt. \tag{3.19}$$

Equation 3.17, however, cannot be solved analytically. For large t, $F \to 1$ (see equation 3.5). When $\tau_F \ll \tau_D$, the synapse is depression dominated, and $D \to \frac{1}{k\tau_D t}$ (see equation 3.9, replacing p with $F \to 1$). Therefore when $\tau_F \ll \tau_D$, we have

$$s \to \frac{\tau_a}{\tau_D}, \tag{3.20}$$

the same long time limit as that for a synapse with pure STD.

We solve equation 3.17 numerically and show the time evolution of facilitation factor F, depression factor D, and gating variable s in Figure 3 for different model parameters. The top row of Figure 3 shows the dependence of synaptic dynamics on α. Note that here, we illustrate a depression-dominated synapse. We see that with a larger α, the increase of F and the decrease of D with time become faster, and s has a larger maximum and reaches its maximum faster (see panels A1–A3 in Figure 3). Modulating α does not qualitatively change the synaptic dynamics (the same conclusion still holds for a facilitation-dominated synapse). We also see that the long time limit of s does not depend on α (see panel A3 in Figure 3), as equation 3.20 suggests.

The dependence of synaptic dynamics on the facilitation time constant τ_F for a facilitation-dominated synapse is shown in the middle row of Figure 3. With a larger τ_F, the increase of F and s and the decrease of D become faster (see panels B1–B3 in Figure 3). When $\tau_F \gg \tau_D$, D and s become insensitive to the value of τ_F (see the blue and green curves in panels B2 and B3, Figure 3). We see that after a period of rapid increase, the activation level of the gating variable s for a facilitation-dominated synapse increases much more slowly

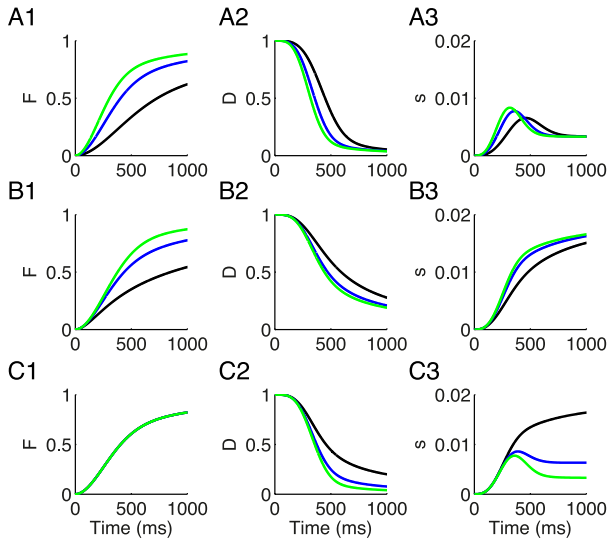

Figure 3: Activation level of a synapse with both STF and STD. (A1–A3) The time evolution of facilitating factor F (A1), depressing factor D (A2), and gating variable s (A3) for different α (green, 0.4; blue, 0.25; black, 0.1). (B1–B3) The time evolution of F (B1), D (B2), and s (B3) for different τ_F (green, 600 ms; blue, 300 ms; black, 100 ms). (C1–C3) The time evolution of F (C1), D (C2), and s (C3) for different τ_D (green, 600 ms; blue, 300 ms; black, 100 ms). Parameters used: $k = 50$ sec^{-2}, $\tau_a = 2$ ms. In A1 to A3, $\tau_F = 400$ ms, $\tau_D = 600$ ms. In panels B1 to B3, $\tau_D = 100$ ms, $\alpha = 0.25$. In panels C1 to C3, $\tau_F = 400$ ms, $\alpha = 0.25$.

than that for a synapse with pure STF (compare the blue curves in Figure 1 D and in panel B3, Figure 3). For a depression-dominated synapse, D and s depend only weakly on τ_F (data not shown). The bottom row in Figure 3 shows the dependence of synaptic dynamics on the depression time constant τ_D. We see that the facilitation factor F is independent of τ_D (see panel C1 in Figure 3) by design (see equation 3.16), while the depression factor D decreases faster with a larger τ_D (see panel C2 in Figure 3). Interestingly, the gating variable s shows a transition from facilitation dominance to depression dominance when τ_D increases from a value much smaller than τ_F to a value much larger than τ_F (see the black and green curves in panel C3, Figure 3). Therefore, the interaction of F and D determines whether the synapse is facilitation or depression dominated.

4 Fluctuating Ramping Input

We now consider the case when the ramping input is noisy and is described by equation 2.3, as neurons downstream from a decision circuit will

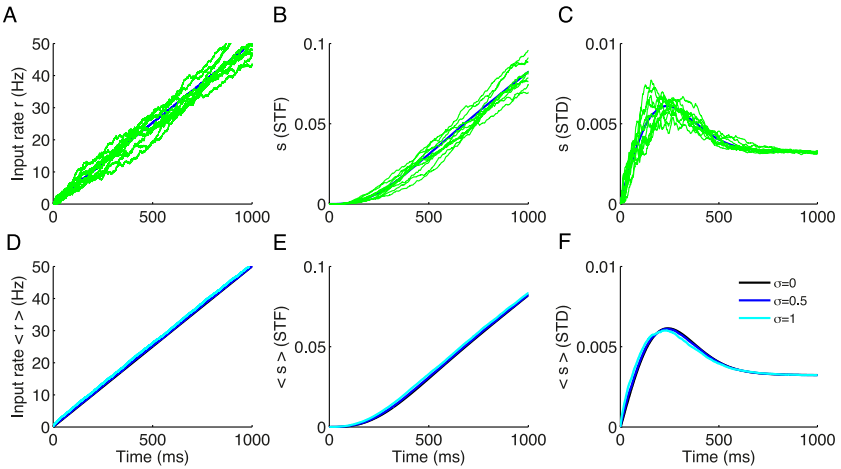

Figure 4: Synaptic activation of a downstream neuron that receives inputs from a population of presynaptic neurons showing ramping activity. (A–C) Fluctuating ramping input described by the drift-diffusion model (A), the activation level s for synapses with pure STF (B), and for synapses with pure STD (C). Blue: the average activity of $r(t)$ (A) and s (B–C) over 300 realizations. Green: illustrated trajectories for 10 realizations. In panels A to C, $\mu = 0.5$ sec^{-1} ($k = 50$ sec^{-2}) and $\sigma = 0.5$ sec^{-1}. (D–F) Ensemble averaged ramping inputs $\langle r \rangle$ (D), activation level $\langle s \rangle = \frac{1}{N} \sum_i s_i$ for synapses with pure STF (E), and pure STD (F) for different noise levels with $\mu = 0.5$, $\sigma = 0,\ 0.5,$ and 1 (in sec^{-1}). N is the size of presynaptic population.

receive. Each downstream neuron receives a summation of inputs from many presynaptic neurons. Since the synaptic efficacy scales with the number of presynaptic neurons, the conductance to a downstream neuron is given by the average gating variables, denoted as $\langle s \rangle$. Here, the angular bracket represents averaging over presynaptic neuronal populations, which is implemented in simulations by averaging different realizations of the noise. The upper row of Figure 4 shows 10 different realizations of $r(t)$ (see panel A), gating variable s for synapses with pure STF (see panel B) and with pure STD (see panel C), and the corresponding averaging values over 300 realizations for $\mu = 0.5$ Hz (i.e., $k = 50$ sec^{-2}).

Figure 4 (lower row) shows the results for $\sigma = 0,\ 0.5,$ and 1 Hz when $\mu = 0.5$ Hz. As one expects, the average ramping input $r(t)$ follows the deterministic trajectory (see Figure 4D). Since equations 2.4 and 2.8 cannot be solved analytically due to the interaction term between $r(t)$ and F or D, we hope the deterministic results obtained in the preceding section can give a good approximation to the average synaptic activation in the low-noise regime, that is, when σ is small. From Figures 4E and 4F, we see that the

deterministic results give a very accurate approximation ($R^2 = 0.999$ and 0.993 in Figure 4E for STF, $R^2 = 0.996$ and 0.944 in Figure 4F, when $\sigma = 0.5$ and 1 sec^{-1}, respectively), even when the noise level is two times the drift term. Therefore, the theoretical results for deterministic ramping input provide a good description for the conductance of downstream neurons receiving ramping inputs described by the drift-diffusion model.

5 Discussion

We investigated the downstream effect of ramping neuronal activity through synapses showing STP. We first derived analytical results for deterministic linear ramping input through synapses displaying pure STF or STD and showed the different synaptic dynamics in contrast to a steady input rate. We obtained a simple approximation for the maximal value of the activation level and the time taken to reach the maximum for a synapse with pure STD. For the general case, when a synapse shows both STF and STD effects, we found that it behaves as a synapse with pure STD when the facilitation time constant τ_F is much smaller than the depression time constant τ_D. We further investigated the dependence of synaptic dynamics on model parameters numerically in the general case. We found a transition from facilitation dominance to depression dominance when τ_D increases from a value much smaller than τ_F to a value much larger than τ_F. A downstream neuron will receive an averaged input from the presynaptic population. We then showed that the averaged synaptic activation level to the downstream neuron is well described by the deterministic solution even when the fluctuation of the ramping input is strong. These results provide insights for downstream impacts of ramping neuronal activity through synapses showing STP.

Cortical areas showing ramping neuronal activity project to other cortical areas and also subcortical areas such as the striatum, thalamus, and superior colliculus. The striatal activity has been observed to ramp up followed by saturation during evidence accumulation when monkeys performed perceptual decision making (Ding & Gold, 2010). Our work showed that this observation could be explained by utilizing STD in the corticostriatal synaptic projection. A direct measurement of EPSP/EPSC for synapses receiving ramping input is not available yet. Our results could be directly tested by intracellular recording in vitro (e.g., using cortical slices), in which a synaptic input ramps over time with a slope that can be parametrically varied. For synapses with STF, our results showed that the activation of gating variable is slower and less sensitive to the ramping slope at the early stage than the control case without STP, followed by the same linear increase as in the control case since $F \to 1$ for large t. For synapses with STD, the ramping slope is encoded only at the initial period of evidence

accumulation and the steady state is insensitive to it. This prediction can be tested in the fixation time version of perceptual decision-making tasks. Therefore, we showed the differential properties of synapses with STF and STD in encoding the slope of ramping activity, which represents the bias of stimulus in making decisions.

One future direction is to include the intrinsic synaptic noise in the deterministic model for STP and investigate its influence when the synapse is driven by fluctuating ramping input. Depressing synapses with intrinsic noise receiving a Poisson input with constant rate have been studied (Rosenbaum, Rubin, & Doiron, 2012, 2013). Synapses displaying STD and stochastic vesicle dynamics were shown to behave as a frequency-dependent filter in signal transmission (Matveev & Wang, 2000; Rosenbaum et al., 2012), in contrast to the broadband signal transmission for deterministic synapses (Lindner et al., 2009), and also influence the transfer of neuronal correlations (Rosenbaum et al., 2013). Extension of our work to include intrinsic synaptic noise will provide further insights into the downstream impact of ramping neuronal activity during perceptual decision making and timing.

Appendix

The Dawson's integral $\mathcal{F}(x)$ is defined as (Abramowitz & Stegun, 1970)

$$\mathcal{F}(x) = e^{-x^2} \int_0^x e^{y^2}\, dy. \tag{A.1}$$

$\mathcal{F}(x)$ has the following asymptotic expansion

$$\mathcal{F}(x) \simeq \frac{1}{2x} + \frac{1}{4x^3} + \dots \tag{A.2}$$

when x is large, and the series expansion

$$\mathcal{F}(x) \simeq x - \frac{2}{3}x^3 + \frac{4}{15}x^5 + \dots \tag{A.3}$$

when x is small (Abramowitz & Stegun, 1970).

For comparison, we present here results for a constant input rate, $r(t) \equiv r$. For a synapse with pure STF, the solutions for equations 2.4 and 2.5 are given by

$$F = \frac{\alpha r \tau_F}{1 + \alpha r \tau_F} + \left(F_0 - \frac{\alpha r \tau_F}{1 + \alpha r \tau_F} \right) \exp\left(-(1 + \alpha r \tau_F) \frac{t}{\tau_F} \right), \tag{A.4}$$

$$s = r \tau_a F. \tag{A.5}$$

For large t,

$$s \to \frac{\alpha r^2 \tau_a \tau_F}{1 + \alpha r \tau_F}. \tag{A.6}$$

For a synapse with pure STD, the solutions of equations 2.8 and 2.9 are given by

$$D = \frac{1}{1 + \tau_D pr} + \left(D_0 - \frac{1}{1 + \tau_D pr} \right) \exp\left(-(1 + \tau_D pr) \frac{t}{\tau_D} \right), \tag{A.7}$$

$$s = pr\tau_a D. \tag{A.8}$$

When t is small (but larger than τ_a),

$$D \simeq 1 - prt. \tag{A.9}$$

When t is large, D and s reach their steady states,

$$D \to \frac{1}{1 + \tau_D pr}, \tag{A.10}$$

$$s \to \frac{pr\tau_a}{1 + \tau_D pr}. \tag{A.11}$$

When $\tau_D pr \gg 1$, that is, $r \gg \frac{1}{\tau_D p} = \frac{1}{0.6 * 0.45} = 3.7$ Hz, this steady state of s is reduced to

$$s \to \frac{\tau_a}{\tau_D}, \tag{A.12}$$

which is independent of the constant input rate r and release probability p and has the same expression as the steady state for a deterministic linear ramping input, equation 3.10.

As a control case, we consider a synapse without STP. Taking $F = 1$ in equation 2.5, then the activation of the synapse is given by

$$s = k\tau_a t + k\tau_a^2 (e^{-t/\tau_a} - 1) + s_0 e^{-t/\tau_a} \tag{A.13}$$

for a ramping input rate $r = kt$ and

$$s = r\tau_a (1 - e^{-t/\tau_a}) + s_0 e^{-t/\tau_a} \tag{A.14}$$

for a constant input rate r.

Acknowledgments

This work was supported by a Swartz Foundation Fellowship (W.W.), and the National Institutes of Health grants R01 MH062349 (X.-J. W).

References

Abbott, L. F., & Regehr, W. G. (2004). Synaptic computation. *Nature*, *431*, 796–803.

Abramowitz, M., & Stegun, I. (1970). *Handbook of mathematical functions with formulas, graphs, and mathematical tables*. New York: Dover.

Ding, L., & Gold, J. I. (2010). Caudate encodes multiple computations for perceptual decisions. *J. Neurosci.*, *30*, 15747–15759.

Fuhrmann, G., Segev, I., Markram, H., & Tsodyks, M. (2002). Coding of temporal information by activity-dependent synapses. *J. Neurophysiol.*, *87*(1), 140–148.

Gold, J. I., & Shadlen, M. N. (2007). The neural basis of decision making. *Annu. Rev. Neurosci.*, *30*, 535–574.

Hanes, D. P., & Schall, J. D. (1996). Neural control of voluntary movement initiation. *Science*, *274*, 427–430.

Hempel, C. M., Hartman, K. H., Wang, X.-J., Turrigiano, G. G., & Nelson, S. B. (2000). Multiple forms of short-term plasticity at excitatory synapses in rat medial prefrontal cortex. *J. Neurophysiol.*, *83*, 3031–3041.

Huk, A. C., & Shadlen, M. N. (2005). Neural activity in macaque parietal cortex reflects temporal integration of visual motion signals during perceptual decision making. *J. Neurosci.*, *25*, 10420–10436.

Komura, Y., Tamura, R., Uwano, T., Nishijo, H., Kaga, K., & Ono, T. (2001). Retrospective and prospective coding for predicted reward in the sensory thalamus. *Nature*, *412*, 546–549.

Lindner, B., Gangloff, D., Longtin, A., & Lewis, J. E. (2009). Broadband coding with dynamic synapses. *J. Neurosci.*, *29*, 2076–2088.

Matveev, V., & Wang, X.-J. (2000). Differential short-term synaptic plasticity and transmission of complex spike trains: To depress or to facilitate? *Cereb. Cortex*, *10*, 1143–1153.

Merchant, H., Harrington, D. L., & Meck, W. H. (2013). Neural basis of the perception and estimation of time. *Annu. Rev. Neurosci.*, *36*, 313–336.

Mita, A., Mushiake, H., Shima, K., Matsuzaka, Y., & Tanji, J. (2009). Interval time coding by neurons in the presupplementary and supplementary motor areas. *Nat. Neurosci.*, *12*, 502–507.

Morrison, A., Diesmann, M., & Gerstner, W. (2008). Phenomenological models of synaptic plasticity based on spike timing. *Biol. Cybern.*, *98*, 459–478.

Ratcliff, R., Cherian, A., & Segraves, M. (2003). A comparison of macaque behavior and superior colliculus neuronal activity to predictions from models of two-choice decisions. *J. Neurophysiol.*, *90*, 1392–1407.

Reutimann, J., Yakovlev, V., Fusi, S., & Senn, W. (2004). Climbing neuronal activity as an event-based cortical representation of time. *J. Neurosci.*, *24*, 3295–3303.

Rosenbaum, R., Rubin, J., & Doiron, B. (2012). Short term synaptic depression imposes a frequency dependent filter on synaptic information transfer. *PLoS Comput. Biol.*, *8*, e1002557.

Rosenbaum, R., Rubin, J. E., & Doiron, B. (2013). Short-term synaptic depression and stochastic vesicle dynamics reduce and shape neuronal correlations. *J. Neurophysiol.*, *109*, 475–484.

Simen, P., Balci, F., de Souza, L., Cohen, J. D., & Holmes, P. (2011). A model of interval timing by neural integration. *J. Neurosci.*, *31*, 9238–9253.

Tsodyks, M. V., & Markram, H. (1997). The neural code between neocortical pyramidal neurons depends on neurotransmitter release probability. *Proc. Natl. Acad. Sci. U.S.A.*, *94*, 719–723.

Tsodyks, M., Pawelzik, K., & Markram, H. (1998). Neural networks with dynamic synapses. *Neural Comput.*, *10*, 821–835.

Wang, X. J. (2002). Probabilistic decision making by slow reverberation in cortical circuits. *Neuron*, *36*, 955–968.

Wang, X.-J. (2008). Decision making in recurrent neuronal circuits. *Neuron*, *60*, 215–234.

Wei, W., Rubin, J. E., & Wang, X.-J. (2015). Role of the indirect pathway of the basal ganglia in perceptual decision making. *J. Neurosci.*, *35*, 4052–4064.

Received August 13, 2015; accepted November 23, 2015.